Synthesis of Ti3SiC2 coatings onto SiC monoliths from molten salts

B Chahhou, C Labrugère-Sarroste, F Ibalot, J Danet, Jérôme Roger

Synthesis of Ti_3SiC_2 coatings onto SiC monoliths from molten salts

B. Chahhou[a], C. Labrugère-Sarroste[b], F. Ibalot[b], J. Danet[a], J. Roger [a,*]

[a] Université de Bordeaux, CNRS, Laboratoire des Composites ThermoStructuraux, UMR 5801, 33600 Pessac, France

[b] Université de Bordeaux, CNRS, PLACAMAT UMS 3626, 33600 Pessac, France

* Corresponding author: e-mail: jerome.roger@lcts.u-bordeaux.fr

Abstract

Coatings with composition close to Ti_3SiC_2 were obtained on SiC substrates from Ti and Si powders with the molten NaCl method. In this work, the growth of coatings by reaction in the salt between monolithic SiC substrates and titanium powder is obtained between 1000 and 1200°C. At 1000°C, a coating of 8 µm thickness is formed in 10 hours whereas a thin coating of 0.5 µm has been grown in 2 hours. A lack in silicon was first found in the coatings prepared at 1100 and 1200°C. For these temperatures, the addition of silicon powder in the melt had a favorable effect on the final composition, which is found very close to the composition of Ti_3SiC_2. The reaction mechanism implies the formation of TiC_x layers in direct contact with the SiC substrate and the presence of more or less important quantities of Ti_3SiC_2 and $Ti_5Si_3C_x$ in the upper layers.

Keywords: Silicon carbide; Ti_3SiC_2; Coating; Synthesis; Molten salt

1. Introduction

MAX phase are ternary layered compounds with the general formula $M_{n+1}AX_n$ formed from at least one transition metal (M), one metalloid element (A) and a non-metal (X) which can be either carbon or nitrogen [1,2]. *n* is an integer value which ranges between 1 and 3 so that only three MAX phase formulae exist according to the nomenclature 211, 312 and 413 [3]. MAX phases are extensively researched because of their unique combination of ceramic and metallic-like properties identified in the 1990s: low density, machinability, excellent thermal and electrical conductivity, thermal-shock resistance, high-temperature oxidation resistance, corrosion resistance, damage tolerance, mechanical strength, and the ability to self-heal [3-8]. Thanks to their damage tolerance and their high temperature properties, MAX phases are serious candidates for high temperature load bearing applications such as jet engines, heating elements and gas burner nozzles [1,3,9-11]. Molten salt method is a quite simple and cost-effective method for synthesis crystalline powders in a low-melting point flux [12]. This process involves the addition of a large amount of molten salt flux to the precursor materials. The molten salt aids synthesis by dissolving reactants and increasing diffusion, [13]. The rapid diffusion rates in molten salts reduce advantageously the synthesis temperature. The use of molten salt also promotes the production of more fine and uniform particles which improve the sinterability [14]. The molten salt method is an efficient technique to use in order to synthesize ceramic powders but it has not been used much for the synthesis of MAX phases [13]. Indeed, some studies reported the production of Cr_2AlC, Ti_2AlC, Ti_3AlC_2 and Ti_3SiC_2 powders in molten salts [14-19]. In 2008, W.B. Tian et al. reported on the creation of Cr_2AlC powders from elemental powders using NaCl-KCl eutectic molten salt heated at temperature between 900 and 1200°C for 1h [14]. Recently, A.M. Abdelkader obtained Cr_2AlC powders from a mixture of Cr_2O_3, Al_2O_3 and graphite powders in NaCl-$CaCl_2$ eutectic mixture at 1200°C for 24h [15]. In 2018, T. Galvin et al. synthesized successfully Ti_2AlC and Ti_3AlC_2 powders from pure elements between 900 and 1300°C in molten NaCl and/or KCl [16]. Quite similarly, L.X. Yang et al. succeeded in synthesizing pure nanosized Ti_3AlC_2 powders from pure elements in the NaCl-KCl eutectic molten salt at 950°C (5h) or 1000°C (2h) [17]. X. Guo et al. formed Ti_3SiC_2 from elemental powders in molten NaCl for a synthesis temperature between 1000 and 1300°C hold for 2h [18]. In this study, silicon was added with an atomic excess of 20% to compensate its volatilization due to the high temperature. The authors investigated the influences of flux/powders weight ratio and reaction temperature on the formed

phases and the morphology of the powders. A practically pure Ti_3SiC_2 powder with a grain size of about 1-2 µm was obtained at 1200°C with 50 wt% NaCl which melts at only 801°C [20]. Not long ago, A. Dash et al. developed a new technic based on molten KBr to synthesis pure micronic Ti_3SiC_2 powder from Ti, Si, Al and C powders by heating between 700 and 1300°C for 1h in the open air [19]. Aluminum was added next to increase the purity of the Ti_3SiC_2 powder. Some studies demonstrated the feasibility of using the low-temperature molten salt synthesis technique in the preparation of metallic carbides coatings on graphite flakes, carbon black particles or carbon fibres [21-24]. These studies used metallic titanium powders in alkali chloride salts at temperatures below 1000°C for a few hours. TiC coatings on graphite flakes were obtained this way with high quality: crack free, homogeneous, and comprising nanosized TiC particles [21,22]. Homogeneous TiC coatings were also prepared on carbon black particles with thickness that could be readily tailored by adjusting the Ti/C ratio of the starting mixture [23]. The reaction of titanium and carbon fibres in molten salts yields also high-quality TiC coatings [24]. Due to its high temperature stability, the Ti_3SiC_2 phase could be an interesting interphase of the SiC_f/SiC composites [25-27] and for assembling SiC-based materials [28-31]. In both cases, it is necessary to obtain a controlled coating on SiC materials. Several technics were employed successfully to form Ti_3SiC_2 coatings. Chemical vapor deposition has been the most popular route taken to make Ti_3SiC_2 films using $SiCl_4$, $TiCl_4$, CCl_4, and H_2 as precursor species at temperatures above 1300°C [32]. Furthermore, good quality Ti_3SiC_2 thin films have been grown at 900°C on a TiC substrate by magnetron sputtering method [33]. Pulsed laser deposition has been used to produce Ti_3SiC_2 coatings at a maximum temperature of 300°C [34]. Ti_3SiC_2 phase was also obtained on SiC fibres via the electrophoretic deposition method with coating thickness ranging from 400 nm to 400 µm [25,26]. Despite these previous works, it would be particularly interesting to have a simple, robust and inexpensive technique for producing Ti_3SiC_2 coatings on SiC substrates. As mentioned above, molten salts were already used for preparing ceramic coatings on ceramic substrates. Growing Ti_3SiC_2 coatings on SiC substrates using a molten salt bath seems to be a promising solution which is discussed in this article.

2. Experimental

2.1 Background on the reaction of titanium with SiC from molten NaCl

Very few articles in the literature deal with the mechanism of ceramics growth by reaction of metallic titanium in a molten salt. Two possible reaction mechanisms were reported during molten salt synthesis: 1) dissolution-precipitation occurs when multiple reactants dissolved in the salt react together and the solid products precipitate out of the salt; 2) the other mechanism involves one or more reactants dissolving in the salt which form the solid products on the surface of the substrate [35]. We could not isolate any source of data relating to the thermodynamics of titanium halides in molten salts. The main source of information is from the article of M.E. Straumanis et al. [36]. This study focused on the titanizing of metallic alloys and ceramic materials in molten NaCl or KCl salts. The authors bring the conclusions that titanium can be transported and react at the metallic state or in the form of $TiCl_2$ and $TiCl_3$ by releasing gaseous sodium (Equations 1 and 2).

$$\boldsymbol{Ti_{(S)} + 2\,NaCl_{(L)} \rightarrow TiCl_{2(L)} + 2\,Na_{(G)}} \qquad \text{Equation 1}$$

$$\boldsymbol{Ti_{(S)} + 3\,NaCl_{(L)} \rightarrow TiCl_{3(L)} + 3\,Na_{(G)}} \qquad \text{Equation 2}$$

The calculated Ti-Si-C phase diagrams at 1000°C, 1100°C and 1200°C are shown in Figure 1. The relevant thermodynamic description of this ternary system reported by Y. Du et al. was used for these calculations with the help of Thermo-Calc software [37,38]. These diagrams highlight the equilibrium between Ti_3SiC_2 and SiC at these temperatures. The normalized driving forces of precipitation for the phases along the SiC-Ti composition line is shown in Figure 2. On the stability composition range of SiC, these calculations show that the normalized driving forces of $TiSi_2$ and Ti_3SiC_2 are quite close, $TiSi_2$ having significantly higher values. The corresponding reaction is given in Equation 3 with $\Delta G_{1000°C}$ = -48.3 kJ and $\Delta G_{1200°C}$ = -46.3 kJ for 1 mole of atoms in the system:

$$\boldsymbol{4\,SiC_{(S)} + 7\,Ti_{(S)} \rightarrow 2\,Ti_3SiC_{2(S)} + TiSi_{2(S)}} \qquad \text{Equation 3}$$

However, J. Xi et al. have recently shown that silicon of SiC can be selectively dissolved by molten fluorinated salts [39]. It can be reasonably considered that molten NaCl could corrode SiC to form silicon chlorides dissolved in the liquid salt. It is also likely that such species evaporate in the form of $SiCl_n$ with n = 2, 3 or 4. The reaction of Equation 4, which leads to the formation of a Ti_3SiC_2 layer, seems to be able to take place, with m = 2 or 3:

$$\boldsymbol{4\,SiC_{(S)} + 6\,TiCl_{m(L)} \rightarrow 2\,Ti_3SiC_{2(S)} + 2\,SiCl_{n(L)} + (3m - n)\,Cl_{2(L)}} \qquad \text{Equation 4}$$

The possibility of obtaining and controlling the growth of a Ti_3SiC_2 layer at the surface of SiC materials by reaction with titanium in the presence of molten NaCl is therefor examined here. That way, the possibility to limit the dissolution of silicon from SiC by adding silicon directly in the molten salt is examined as well.

2.2 Materials and experimental procedures

Commercial titanium powder (44µm, 99% purity, Strem Chemicals, Inc., Germany), silicon powder (44 µm, 99.99% purity, Strem Chemicals, Inc., Germany); and sodium chloride powder (99% purity, Alfa Aesar GmbH & Co KG, Germany) were used. Commercial sintered SiC (1.5% closed porosity, Mersen-Boostec, France) was used as substrate of about 5×5×5 mm^3. The powders mixtures were composed of 1g of titanium with 0, 0.5 or 1g of silicon; and a sufficient amount of NaCl to cover the SiC substrate. An alumina crucible was used (50×20×20 mm^3, 99.7% purity, Sceram Ceramics, France), and the amount of NaCl added was 6.27g. The mixtures used in this study are detailed in Table 1. The heat treatments were performed in a horizontal alumina-tube furnace at normal pressure under a continuous flow (5 $mL.min^{-1}$) of high purity argon (Alphagaz2, AirLiquide, France) in the presence of compacted titanium powder as an oxygen getter. The thermal cycle involved heating and cooling rates of 2°$C.min^{-1}$ and a dwell at 500°C during 1h to eliminate volatile impurities from the salt. The melting and boiling temperature of NaCl being respectively 801°C and 1465°C [20], the reactions were realized at 1000, 1100 or 1200°C during 2 or 10 hours. After the thermal cycle, the crucible was put in water at a temperature between 75 and 90°C to dissolve the salt and to extract the SiC substrate. Several washings were performed to remove salt still present and a filtration was processed to isolate the remaining powder. Coated SiC substrate and remaining powder were dried at 100°C during 2h. The XRD analyses on the coated substrates were performed in the Bragg-Brentano geometry with a Bruker D8 Advance diffractometer using a Cu Kα radiation fitted with a one-dimensional position sensitive silicon strip detector (Bruker, Linxeye). The XRD patterns were recorded using a 2θ step size and range of respectively 0.01° and 10-100° and a counting time of 0.3 second per step. The coated substrates were cross-cut and polished drown to a 1 µm diamond finish. The microstructures were examined with a FEI Quanta 400FEG scanning electron microscopy (SEM) operated at 10 kV. Backscattered electron diffraction (EBSD) data were obtained at 15 kV with a FEG SEM (JEOL JSM 7100F) equipped with an

CMOS Symmetry S2 EBSD detector (Oxford Instruments). For these analyses, the samples were mounted and then polished with a VibroMet™ 2 (Buehler). The atomic compositions of each coating were obtained from an electron probe microanalyzer (EPMA, Cameca SXFive) with wavelength-dispersive spectrometers (WDS). Chemical quantifications of the resulting powders were done by ICP-AES (ICAP 6500, Thermofisher Scientific, USA) for the metallic elements (Ti, Si) and by elementary analyzer (ISA-CNRS, France) for the non-metals (C, O). RF Glow Discharge Optical Emission Spectroscopy (GDOES) (GD-Profiler2, Horiba) has been used to perform depth profiles on the coated samples. Operating conditions were: Ar plasma gas, anode diameter 4 mm, argon pressure 900 Pa, applied RF power 50 W, 300s sputtering duration. Main chemical elements Ti, Si, C were tracked as well as O, Na, Cl. A MAHR mechanical profilometer was used to monitor the crater depth in order to convert time into microns. The optical intensity was converted into atomic percentage with a calibration performed on SiC and Ti matrix standards.

3. Results and discussion

3.1 Effect of the temperature on formation of a coating

The metallographic sections of the SiC substrates heat-treated at 1000, 1100 or 1200°C for 2h in molten NaCl in presence of Ti powder are presented in Figures 3. The average thickness of the coating heated at 1000°C for 2 hours is equal to 0.5±0.1 µm, this sample is called TSC1. For a heating at 1000°C for 10 hours, the average thickness of the coating is 8±1 µm (TSC2). At 1100°C (TSC3) and 1200°C (TSC4), coatings are obtained with average thicknesses equal to 9±1 and 20±1 µm, respectively. These coatings appear quite homogeneous with some small porosities. Despite some cracks and pores, they are well adherent on the SiC substrate and they are composed of submicronic grains. SEM micrographs and atomic concentration mappings of these samples are shown in Figures 4. They show that all the coatings are polyphase. The homogeneous presence of titanium in all the coatings is evidenced. It is to note the presence of a layer in direct contact with the substrate containing a very small amount of silicon, the thickness of which increases with temperature. The corresponding XRD patterns are shown in Figure 5. Depending on the thickness of the coating, the SiC substrate is detected. For the sample heated at 1000°C, the coating contains TiC_x and Ti_5Si_3 phases. The presence of Ti_3SiC_2 is not clearly evidenced but this could be explained by the low intensity of its diffraction peaks, the smallness of its grains and a

poor crystallization at these relatively low temperatures. The coatings at 1100°C and 1200°C contain a large quantity of TiC_x with smaller amounts of Ti_5Si_3 and probably Ti_3SiC_2. The intensities of the peaks were too low to determine the ratios of these phases. The average atomic ratios from EDS analyses realized on a wide surface of the coatings were found to be Ti:Si:C = 48:22:30 for TSC2 ; Ti:Si:C = 52:11:37 for TSC3 and; Ti:Si:C = 53:11:36 for TSC4, respectively. The accuracy of the measurement being of ±1%. The chemical compositions of the layers are quite close to the expected atomic ratio Ti:Si:C = 50.0:16.7:33.3. It should be noted that the percentage of oxygen within the coatings was measured between 3 and 6 at.% for all the samples of this study. This pollution could come from the oxides at the surface of the starting materials or to an oxidation at the contact with the air. The positions of the measured compositions along the width of each coating are reported by orange points in the phase diagrams in Figures 1. The average compositions obtained on a wide section of each coating are also reported on Figures 1, they are indicated by blue five-pointed stars. The dispersion of the points confirms that the coatings are mainly composed of the phases in the TiC_x-$Ti_5Si_3C_x$-Ti_3SiC_2 triangle. At 1000°C, the presence of $TiSi_2$ and TiSi seems to be possible but it was not clearly identified by X-ray diffraction maybe because of too low quantities. These results confirm that the SiC substrate reacts with titanium in presence of molten NaCl. The thickness of the coatings increases with the temperature. The composition of the coatings at 1100°C and 1200°C are quite similar with important quantities of TiC_x because of a lack of silicon in these coatings compared to the composition of Ti_3SiC_2. Conversely, the coating at 1000°C contains a little excess in silicon but its composition is very close to the composition of Ti_3SiC_2. The chemical composition gradients through each coating reveal that the growth mechanism of the coatings includes a first layer of TiC_x formed directly in contact with the substrate. This layer is visible on the BSE images in Figures 3 and Figures 4. Closer to the surface of the coatings, the composition gets very close to Ti_3SiC_2. It can be deduced that the general composition gradient is SiC/TiC_x/Ti_3SiC_2+($Ti_5Si_3C_x$, TiSi, $TiSi_2$). Each layer is found in thermodynamic equilibrium with the neighboring layers. These first results evidenced that the reaction between SiC and titanium in molten NaCl promotes the growth of TiC_x phases because of a lack of silicon particularly at 1100 and 1200°C. It is then deduced that silicon is dissolved in the liquid salt during the reaction. This behaviour is not evidenced when SiC is heat-treated in pure NaCl at 1200°C (SC sample), as shown in Figure 6. The chemical composition at the surface of the SiC substrate was found unchanged. This confirms that the growth of TiC_x is not induced by a salt corrosion of the SiC substrate with dissolution of silicon. The

predominant formation of TiC_x and $Ti_5Si_3C_x$ phases from compacted Ti, Si and C powders as starting materials was already reported during reactive pressureless sintering of Ti_3SiC_2 [40]. Very low quantities of the MAX phase were obtained, excepted when sufficient Al contents were added because it accelerates the reaction between the TiC and Ti_5Si_3 phases. The reaction route proposed by the authors implies 3 stages: first, Ti reacts with C to form TiC; secondly, Ti reacts with Si to form Ti_5Si_3; finally, TiC and Ti_5Si_3 react together to produce Ti_3SiC_2. TiC and Ti_5Si_3 are considered as intermediate phases on the way to form the MAX phase. It is therefore not surprising that the same phases are formed in the coatings of the present study. In the study by T. Galvin et al., small amounts of TiC_x were also present beside Ti_2AlC and Ti_3AlC_2 synthesized with NaCl or KCl flux from elemental powders [16]. The authors identified that the growth of Ti_2AlC begins with TiC_x growth on graphite flakes. According to these previous studies, the mechanism of Ti_3SiC_2 growth from the reaction between SiC and Ti in molten NaCl probably has as a first step the formation of the TiC_x and Ti_5Si_3 phases. The corresponding reactions are given in Equations 5 and 6 with, respectively, $\Delta G_{1200°C}$ = -45.1 kJ and $\Delta G_{1200°C}$ = -42.6 kJ for 1 mole of atoms. From these values, the formation of TiC appears to be a little more favourable. This is confirmed by the normalized driving forces shown in Figure 2-c); TiC_x has slightly higher values than $Ti_5Si_3C_x$. It should be noticed that TiC_x has the highest driving force when pure metallic titanium is present. This is in accordance with the preferentially formation of TiC_x phase at the beginning of the reaction.

$$\boldsymbol{SiC_{(S)} + Ti_{(S)} \rightarrow TiC_{(S)} + Si_{(S)}} \qquad \text{Equation 5}$$

$$\boldsymbol{3\,SiC_{(S)} + 5\,Ti_{(S)} \rightarrow Ti_5Si_{3(S)} + 3\,C_{(S)}} \qquad \text{Equation 6}$$

Larger amounts of silicon than expected are probably dissolved in the molten salt, which justifies the lack of silicon in the final coatings. It must be possible to limit these losses by adding silicon to the melt. The formation of the Ti_5Si_3 occurs also according to Equation 7 with $\Delta G_{1200°C}$ = -71.9 kJ for 1 mole of atoms.

$$\boldsymbol{3\,Si_{(S)} + 5\,Ti_{(S)} \rightarrow Ti_5Si_{3(S)}} \qquad \text{Equation 7}$$

The formation of the $TiSi_2$ occurs also according to Equation 8 with $\Delta G_{1200°C}$ = -55.8 kJ for 1 mole of atoms.

$$\boldsymbol{2\,Si_{(S)} + Ti_{(S)} \rightarrow TiSi_{2(S)}} \qquad \text{Equation 8}$$

The Gibbs energy of formation of Ti_3SiC_2 from TiC, Ti_5Si_3 and C (Equation 9) is $\Delta G_{1200°C}$ = -22.2 kJ for 1 mole of atoms.

$$\mathbf{4\ TiC_{(S)} + Ti_5Si_{3(S)} + 2\ C_{(S)} \rightarrow 3\ Ti_3SiC_{2(S)}} \qquad \text{Equation 9}$$

The Gibbs energy of formation of Ti_3SiC_2 from TiC and $TiSi_2$ (Equation 10) is $\Delta G_{1200°C}$ = -40.9 kJ for 1 mole of atoms.

$$\mathbf{2\ TiC_{(S)} + TiSi_{2(S)} \rightarrow Ti_3SiC_{2(S)} + Si_{(S)}} \qquad \text{Equation 10}$$

The calculated Gibbs energies at 1200°C confirm that the formation reactions of TiC and Ti_5Si_3 or $TiSi_2$ (Equations 5, 7 and 8) have higher reactivities than the final reaction between them to form the MAX compound (Equations 9 and 10). All the coatings contain more of less quantities of TiC_x whose growth could be limited by adding silicon to the salt. For this, the most promising condition is obtained at 1200°C as it promotes the growth of the thickest coating despite a silicon defect. The coating formed at 1000°C seems less interesting for this approach as its quantity of TiC_x is the lowest, its average composition is slightly in excess of silicon; and its thickness is the lowest.

3.2 Effect of the composition at 1200°C on formation of Ti_3SiC_2 phase

The metallographic sections of the SiC substrates heated at 1200°C for 2h in molten NaCl containing Ti and Si powders are shown in Figures 7. The average thicknesses of the samples prepared with 0.5g of Si (TSC5) or with 1g of Si (TSC6) in the salt are equal to 7.0±0.5 µm and 5.0±0.5 µm, respectively. These thicknesses are smaller compared to the coating's thickness of the sample heated at 1200°C with only addition of Ti powder (i.e. 20±1 µm) (TSC4). SEM micrographs and EDS mappings of these samples are shown in Figures 8. These coatings are adherent on the substrates and they seem more homogeneous than the coating without silicon in the melt. The coatings with Si addition are composed of two layers. From XRD (Figure 5), the compositions of the coatings are greatly affected by Si addition in the salt. Indeed, for 0.5g of Si (TSC5) in the melt, the main peaks correspond to Ti_5Si_3 and some small peaks correspond to Ti_3SiC_2. For 1g of Si in the melt (TSC6), the peaks of TiC_x and Ti_5Si_3 are very low, and the most intense peaks correspond to the SiC substrate. The formation of Ti_3SiC_2 is not evidenced for this sample probably because of the weakness of its diffraction peaks. High magnifications images (x10000) and the EDS quantifications in Figures 7-b,d) show that the coatings of the samples are composed of similar layers with different thicknesses. These coatings are composed of a thin TiC_x layer

in contact with the SiC substrate; a layer of Ti_3SiC_2 with a higher thickness for the sample with 0.5g of Si in the melt and an upper $Ti_5Si_3C_x$ layer with traces of TiC_x for the sample with 1g of Si in the melt. The EBSD mapping of the samples prepared from melts with 0.5g and 1g of Si are shown in Figures 9. The Kikuchi patterns presented in insets of Figures 9-a) and 9-b) are attributed to the hexagonal structure of Ti_3SiC_2, which confirm the presence of Ti_3SiC_2 phase between the TiC_x and the $Ti_5Si_3C_x$ layers. These analyses confirm the layered structures for 0.5g and 1g of Si in the melt observed in Figures 7. These layered structures are $SiC/TiC_x/Ti_3SiC_2/Ti_5Si_3C_x$ for 0.5g of Si in the melt; and $SiC/TiC_x/Ti_3SiC_2/Ti_5Si_3C_x+TiC_x$ for 1g of Si in the melt. The lower thicknesses of the coatings formed from the melts containing Si addition could be explained by a lower diffusion of the titanium atoms in the main phases i.e. $Ti_5Si_3C_x$ and Ti_3SiC_2. Without silicon in the starting melt at 1200°C, the main phase in the coating is TiC_x. The diffusion of titanium atoms is higher in this phase. The smallness of the Ti_3SiC_2 layer with addition of 1g of Si can justify the fact that this phase was not detected by X-ray diffraction. The atomic compositions of each coating obtained from the EDS and WDS quantifications along the width of each coating are respectively reported by orange and green points in Figures 10. The atomic compositions of the Ti and Si starting mixtures in molten salts are Ti:Si = 54:46 and Ti:Si = 37:63 for an addition of 0.5 and 1g of Si, respectively. The corresponding composition lines between these mixtures and SiC are drawn in blue dotted lines in Figures 10. The average atomic compositions obtained by EDS realized on a wide surface of the coatings were found to be Ti:Si:C = 53:11:36 for TSC4; Ti:Si:C = 49:20:31 for TSC5 and; Ti:Si:C = 50:16:34 for TSC6. These values correspond to the blue five-pointed stars in Figures 10. The average atomic compositions obtained by WDS realized along lines crossing the coatings were found to be Ti:Si:C = 58:15:27 for TSC4; Ti:Si:C = 52:24:24 for TSC5 and; Ti:Si:C = 50:18:32 for TSC6. These values are localized by blue saint Andrew's crosses in Figures 10. The effect of silicon addition is clearly shown in Figures 10 with an increase of the silicon fraction in the coatings. It is to note that the average compositions of the coating obtained with addition of 1g of silicon is very close to the Ti_3SiC_2 stoichiometry although this coating is mainly composed of $Ti_5Si_3C_x$ and TiC_x with a small amount of Ti_3SiC_2. This fact can be explained by: i) the composition of TiC_x in the first layer which is C-rich ($x\approx1$) because it is in equilibrium with the SiC substrate and ii) the $Ti_5Si_3C_x$ layer is also C-rich ($x\approx1$) because it is in equilibrium with Ti_3SiC_2. The GDOES profiles of the three samples heated at 1200°C are shown in Figures 11-a,b,c). In these figures, the positions of the layers are indicated by vertical dotted lines with an accuracy of ±1µm. The corresponding atomic compositions

obtained from GDOES analyses in the thickness of each coating are indicated by orange points and the average compositions of the coatings are indicated by blue five-pointed stars in Figures 11-d,e,f). The average atomic compositions obtained from GDOES for an analysed surface of 4mm^2 were found to be Ti:Si:C = 58:18:24 for TSC4; Ti:Si:C = 51:24:25 for TSC5 and; Ti:Si:C = 49:17:34 for TSC6. These analyses confirm the compositions identified for each sample. It appears clearly that the addition of silicon in the salt promotes an average composition closer to the expected composition of Ti_3SiC_2. The ICP quantification of the remaining powders obtained after dissolution of the salt for the samples TSC4 and TSC6 are given in Table 2. For both samples, a noticeable quantity of oxygen was measured which is probably induced by reactions with water. The unidentified masses are obviously attributable to the remaining sodium and chlorine. In the case of the sample TSC4, a noticeable quantity of silicon is present in the residual powder whereas no silicon was initially added in the powder mixture. This confirms that a part of the silicon of the SiC substrate is dissolved in the melt which induces the lack of silicon in the coating. The composition of the residual powder from the TSC6 sample shows that the atomic Si/Ti ratio is equal to 1.4. This ratio is lower than the starting value which was 1.7. This indicates that a noticeable part of the silicon was eliminated during the aqueous dissolution of the salt. This entails also that silicon forms compounds with Na and/or Cl which are hydrolysed and eliminate. It is highly probable that the same mechanism also occurs with titanium but to a lesser extent. The X-ray patterns of both powders reveal also the presence of $TiSi_2$, TiSi and Ti_5Si_3 with many others phases that were not clearly identified. These patterns are not given here because of their complexity, several peaks could not be indexed. The formations of Ti_5Si_3, TiSi or $TiSi_2$ powders in the flux is thermodynamically possible as the corresponding reactions induce strong decreases of the Gibbs energy. Indeed, the Gibbs energy variation of $TiSi_2$ formation (Equation 8) is $\Delta G_{1200°C}$ = -55.8 kJ for 1 mole of atoms. The Gibbs energy variation for TiSi formation is calculated to $\Delta G_{1200°C}$ = -71.4 kJ for 1 mole of atoms (Equation 11). One found the value $\Delta G_{1200°C}$ = -74.8 kJ for 1 mole of atoms forming Ti_5Si_4 (Equation 12). The Gibbs energy variation for Ti_5Si_3 (Equation 7) is given herein.

$$\boldsymbol{Ti_{(S)} + Si_{(S)} \rightarrow TiSi_{(S)}} \qquad \text{Equation 11}$$

$$\boldsymbol{5\,Ti_{(S)} + 4\,Si_{(S)} \rightarrow Ti_5Si_{4(S)}} \qquad \text{Equation 12}$$

The formation of these titanium silicides in the salt is thermodynamically favourable and it implies a decrease of the titanium activity. At this time, the calculation of its value in not possible because it is

equal to the activity of titanium dissolved in molten NaCl according to Equations 1 and 2. No thermodynamic data about titanium species formed in liquid NaCl were found in the literature. The decrease of Ti activity explains the decrease of reactivity towards SiC. The addition of silicon in the melt promotes obviously the growth of Ti_3SiC_2 coatings. Addition of silicon probably limits both the losses by dissolution and the reactivity of titanium. The limitation of Ti reactivity is correlated to the lower thicknesses obtained and the presence of titanium silicides in the salt. Finally, the growth of Ti_3SiC_2 coatings assisted by molten salts is evidenced on SiC materials. The mechanism induced by the use of molten NaCl is partly understood and will require further investigation.

4. Conclusion

Coatings on SiC substrates were successfully synthesized between 1000°C and 1200°C by reaction of SiC with titanium and silicon powder in molten baths of NaCl. The thickness and the composition of the produced coatings depends on the temperature and the amount of silicon in the melt. Without silicon in the starting melt, the coating is mainly composed of TiC_x and $Ti_5Si_3C_x$ phases with small amounts of Ti_3SiC_2. A lack in silicon was evidenced at 1100°C and 1200°C by the predominant formation of the TiC_x phase. The addition of silicon in the melt at 1200°C promotes the growth of a coating containing TiC_x, $Ti_5Si_3C_x$ and Ti_3SiC_2 phases. The thickness of the layer of Ti_3SiC_2 is more important for 0.5g of Si in the melt. For 1g of Si in the melt the main phase in the coating is $Ti_5Si_3C_x$. The use of molten salts is a promising way of growing coatings composed of Ti_3SiC_2 formed from SiC substrates.

Acknowledgement

Special thanks to the Région Nouvelle-Aquitaine and the Ministère de l'Enseignement Supérieur et de la Recherche for funding this research.

The authors wish to thank Muriel Alrivie from the Laboratory of ThermoStructural Composites (LCTS - UMR 5801 - UB-CNRS-CEA-SAFRAN) and Arnaud Proietti from the Centre de microcaractérisation Raimond Castaing (UMS 3623) for their kind assistance.

References

[1] M.W. Barsoum, $M_{n+1}AX_n$ phases: a new class of solids; thermodynamically stable nanolaminates, Prog. Solid State Chem., 28 (2000) 201-281, https://doi.org/10.1016/S0079-6786(00)00006-6

[2] M.W. Barsoum, T. El-Raghy, The MAX phases: unique new carbide and nitride materials: tertiary ceramics are soft and machinable, yet heat-tolerant, strong and lighweight, Am. Sci., 89 (2001) 334-343, https://doi.org/10.1511/2001.4.334

[3] M.W. Barsoum, MAX Phases: Properties of Machinable Ternary Carbides and Nitrides, Wiley-VCH Verlag GmbH & Co. KGaA, Weinheim, Germany, 2013, https://doi.org/10.1002/9783527654581

[4] Z.M. Sun, Progress in research and development on MAX phases: a family of layered ternary compounds, Int. Mater. Rev., 56 (2011) 143-166, https://doi.org/10.1179/1743280410Y.0000000001

[5] M.W. Barsoum, M. Radovic, Elastic and mechanical properties of the MAX phases, Annu. Rev. Mater. Res., (2011) 195-227, https://doi.org/10.1146/annurev-matsci-062910-100448

[6] M.W. Barsoum, T. El-Raghy, C.J. Rawn, W.D. Porter, H. Wang, E.A. Payzant, C.R. Hubbard, Thermal properties of Ti_3SiC_2, J. Phys. Chem. Solids, 60 (1999) 429-439, https://doi.org/10.1016/S0022-3697(98)00313-8

[7] T. Zhen, M.W. Barsoum, S.R. Kalidindi, Effects of temperature, strain rate and grain size on the compressive properties of Ti_3SiC_2, Acta Mater., 53 (2005) 4163-4171, https://doi.org/10.1016/J.ACTAMAT.2005.05.020

[8] M. Radovic, M.W. Barsoum, MAX phases: bridging the gap between metals and ceramics, Am. Ceram. Soc. Bull., 92 (2013) 20-27.

[9] M. Radovic, M.W. Barsoum, T. El-Raghy, S.M. Wiederhorn, Tensile creep of coarse grained Ti_3SiC_2 in the 1000-1200°C temperature range, J. Alloys. Compd., 361 (2003) 299-312, https://doi.org/10.1016/S0925-8388(03)00435-3

[10] M. Radovic, M. Barsoum, T. El-Raghy, S. Wiederhorn, Tensile creep of fine grained (3-5 μm) Ti_3SiC_2 in the 1000-1200°C temperature range, Acta Mater., 49 (2001) 4103-4112, https://doi.org/10.1016/S1359-6454(01)00243-9

[11] M. Sundberg, G. Malmqvist, A. Magnusson, T. El-Raghy, Alumina forming high temperature silicides and carbides, Ceram. Int., 30 (2004) 1899-1904, https://doi.org/10.1016/j.ceramint.2003.12.046

[12] Y. Wang, J. Ma, J. Tao, X. Zhu, J. Zhou, Z. Zhao, L. Xie, H. Tian, Synthesis of $CaWO_4$ nanoparticles by a molten salt method, Mater. Lett., 60 (2006) 291-293, https://doi.org/10.1016/j.matlet.2005.08.037

[13] T. Kimura, Molten Salt Synthesis of Ceramic Powders, in: C. Sikalidis (Ed.), Advances in Ceramics - Synthesis and Characterization, Processing and Specific Applications, InTech, 2011, pp. 75-100.

[14] W.B. Tian, P.L. Wang, Y.M. Kan, G.J. Zhang, Cr_2AlC powders prepared by molten salt method, J. Alloys Compd., 461 (2008) 6-11, https://doi.org/10.1016/j.jallcom.2007.06.094

[15] A.M. Abdelkader, Molten salts electrochemical synthesis of Cr_2AlC, J. Eur. Ceram. Soc., 36 (2016) 33-42, http://dx.doi.org/10.1016/j.jeurceramsoc.2015.09.003

[16] T. Galvin, N.C. Hyatt, W.M. Rainforth, I.M. Reaney, D. Shepherd, Molten salt synthesis of MAX phases in the Ti-Al-C system, J. Eur. Ceram. Soc., 38 (2018) 4585–4589, https://doi.org/10.1016/j.jeurceramsoc.2018.06.034

[17] L.X. Yang, Y. Wang, H.L. Zhang, H.J. Liu, C.L. Zeng, A simple method for the synthesis of nanosized Ti_3AlC_2 powder in NaCl–KCl molten salt, Mater. Res. Lett., 7 (2019) 361-367, https://doi.org/10.1080/21663831.2019.1613695

[18] X. Guo, J. Wang, S. Yang, L. Gao, B. Qian, Preparation of Ti_3SiC_2 powders by the molten salt method, Mater. Lett., 111 (2013) 211-213, https://doi.org/10.1016/j.matlet.2013.08.077

[19] A. Dash, Y.J. Sohn, R. Vaßen, O. Guillon, J. Gonzalez-Julian, Synthesis of Ti_3SiC_2 MAX phase powder by a molten salt shielded synthesis (MS3) method in air, J. Eur. Ceram. Soc., 39 (2019) 3651-3659, https://doi.org/10.1016/j.jeurceramsoc.2019.05.011

[20] D. Lide, Physical constants of inorganic compounds, In: CRC Handbook of Chemistry and Physics: CRC Press, 2006.

[21] X. Liu, S. Zhang, Low-temperature preparation of titanium carbide coatings on graphite flakes from molten salts, J. Am. Ceram. Soc., 91 (2008) 667-670, https://doi.org/10.1111/j.1551-2916.2007.02184.x

[22] X. Liu, Z. Wang, S. Zhang, Molten salt synthesis and characterization of titanium carbide-coated graphite flakes for refractory castable applications, Int. J. Appl. Ceram. Technol., 8 (2011) 911-919, https://doi.org/10.1111/j.1744-7402.2010.02529.x

[23] J. Ye, R.P. Thackray, W.E. Lee, S. Zhang, Microstructure and rheological properties of titanium carbide-coated carbon black particles synthesised from molten salt, J. Mater. Sci., 48 (2013) 6269-6275, https://doi.org/10.1007/s10853-013-7424-4

[24] L. Constantin, L. Fan, M. Pouey, J. Roger, B. Cui, J.F. Silvain, Y. Feng Lu, Spontaneous formation of multilayer refractory carbide coatings in a molten salt media, Proc. Natl. Acad. Sci. USA PNAS, 118 (2021) e2100663118, https://doi.org/10.1073/pnas.2100663118

[25] I. Filbert-Demut, N. Travitzky, G. Motz, I. Zhitomirsky, P. Greil, Polymer derived ceramics reinforced with Ti_3SiC_2 coated SiC fibers: A feasibility study, Mater. Lett., 145 (2015) 229-231, https://doi.org/10.1016/j.matlet.2015.01.128

[26] H.G. Lee, D. Kim, Y.S. Jeong, J.Y. Park, W.J. Kim, Formation of Ti_3SiC_2 interphase of SiC fiber by electrophoretic deposition method, J. Korean Ceram. Soc., 53 (2016) 87-92, http://dx.doi.org/10.4191/kcers.2016.53.1.87

[27] S. Li, N. Ni, B. Wu, C. Li, Q. Ding, Z. He, Ti_3SiC_2 interphase coating in SiC_f/SiC composites: Effect of the coating fabrication atmosphere and temperature, J. Eur. Ceram. Soc., 41 (2021) 5820-5862, https://doi.org/10.1016/j.jeurceramsoc.2021.03.058

[28] P. Tatarko, V. Casalegno, C. Hu, M. Salvo, M. Ferraris, M.J. Reece, Joining of CVD-SiC coated and uncoated fibre reinforced ceramic matrix composites with pre-sintered Ti_3SiC_2 MAX phase using Spark Plasma Sintering, J. Eur. Ceram. Soc., 36 (2016) 3957-3967, https://doi.org/10.1016/j.jeurceramsoc.2016.06.025

[29] A. Septiadi, P. Fitriani, A.S. Sharma, D.H. Yoon, Low pressure joining of SiC_f/SiC composites using Ti_3AlC_2 or Ti_3SiC_2 MAX phase tape, J. Korean Ceram. Soc., 54 (2017) 340-348, https://doi.org/10.4191/kcers.2017.54.4.08

[30] X. Zhou, Y. Li, Y. Li, Z. Liu, H. Yang, S. Ding, Y.H. Han, J. Lee, S. Du, Q. Huang, Residual thermal stress of SiC/Ti_3SiC_2/SiC joints calculation and relaxed by postannealing, Int. J. Appl. Ceram. Technol., 15 (2018) 1157-1165, https://doi.org/10.1111/ijac.12900

[31] G. Liu, X. Zhang, J. Yang, G. Qiao, Recent advances in joining of SiC-based materials (monolithic SiC and SiC_f/SiC composites): Joining processes, joint strength, and interfacial behavior, J. Adv. Ceram., 8 (2019) 19-38, https://doi.org/10.1007/s40145-018-0297-x

[32] T. Goto, T. Hirai, Chemically vapor deposited Ti_3SiC_2, Mat. Res. Bull., 22 (1987) 1195-1201, https://doi.org/10.1016/0025-5408(87)90128-0

[33] J.P. Palmquist, U. Jansson, T. Seppanen, P.A. Persson, J. Birch, L. Hultman, P. Isberg, Magnetron sputtered epitaxial single-phase Ti_3SiC_2 thin films, Appl. Phys. Lett. 81, 835 (2002); https://doi.org/10.1063/1.1494865

[34] J.J. Hu, J.E. Bultman, S. Patton, J.S. Zabinski, Pulsed laser deposition and properties of $M_{n+1}AX_n$ phase formulated Ti_3SiC_2 thin films, Tribo. Lett., 16 (2004) 113-122, https://doi.org/10.1023/B:TRIL.0000009721.87012.45

[35] M.L. Hand, M.C. Stennett, N.C. Hyatt, Rapid low temperature synthesis of a titanate pyrochlore by molten salt mediated reaction, J. Eur. Ceram. Soc., 32 (2012) 3211-3219, https://doi.org/10.1016/j.jeurceramsoc.2012.04.046

[36] M. E. Straumanis, S. T. Shih, A. W. Schlechten, The mechanism of deposition of titanium coatings from fused salt baths, J. Electrochem. Soc., 104 (1957) 17-20, https://doi.org/10.1149/1.2428485

[37] Y. Du, J.C. Schuster, H.J. Seifert, F. Aldinger, Experimental investigation and thermodynamic calculation of the titanium–silicon–carbon system, J. Am. Ceram. Soc. 83 (2000) 197-203. https://doi.org/10.1111/j.1151-2916.2000.tb01170.x

[38] J.O. Andersson, T. Helander, L. Höglund, P.F. Shi, B. Sundman, Thermo-Calc and DICTRA, Calphad 26 (2002) 273-312. https://doi.org/10.1016/S0364-5916(02)00037-8

[39] J. Xi, H. Jiang, C. Liu, D. Morgan, I. Szlufarska, Corrosion of Si, C, and SiC in molten salt, Corros. Sci., 146 (2019) 1-9, https://doi.org/10.1016/j.corsci.2018.10.027

[40] B. Xu, Q. Chen, X. Li, C. Meng, H. Zhang, M. Xu, J. Lia, Z. Wang, C. Deng, Synthesis of single-phase Ti_3SiC_2 from coarse elemental powders and the effects of excess Al, Ceram. Inter., 45 (2019) 948-953, https://doi.org/10.1016/j.ceramint.2018.09.270

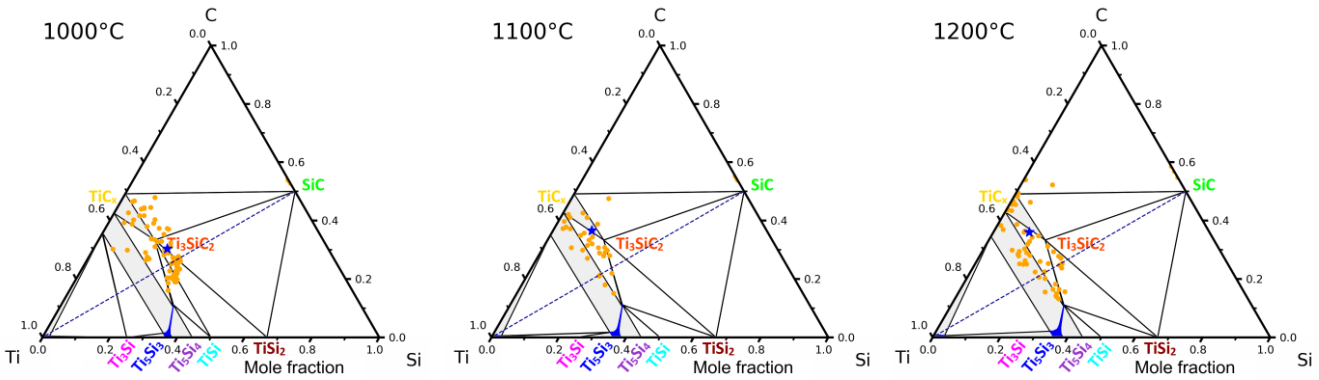

a) b) c)

Figures 1. Localization in the calculated Ti-Si-C phase diagram of the EDS measurements on SiC monoliths heated: a) at 1000°C for 10h; b) 1100°C for 2h and c) 1200°C for 2h. The concentration profiles in dotted lines in Figures 3 are reported here [37,38]. The mean compositions are localized by blue five-pointed stars.

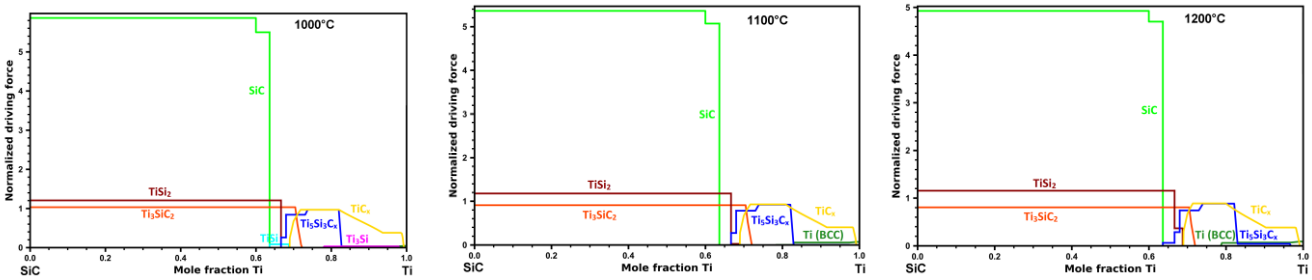

a) b) c)

Figures 2. Driving forces of formation of the phases along the SiC-Ti isopleth at: a) 1000°C, b) 1100°C, and c) 1200°C [37,38].

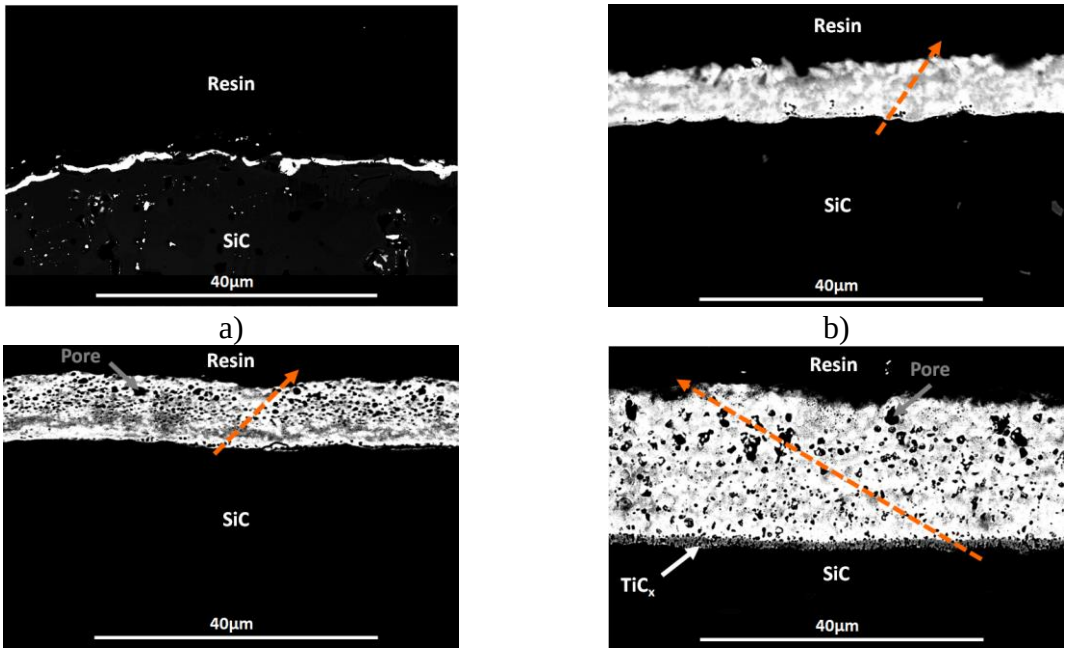

a) b)

c) d)

Figures 3. BSE images of the samples heated at: a) 1000°C during 2h (TSC1), b) 1000°C during 10h (TSC2), c) 1100°C (TSC3), and d) 1200°C (TSC4).

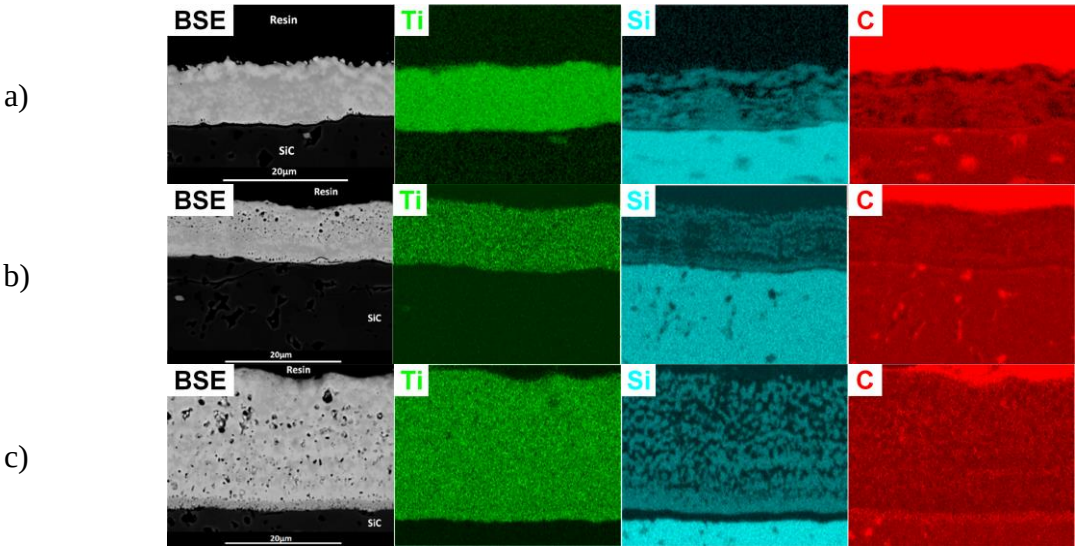

Figures 4. Backscattered electron micrograph and EDS mapping for Ti, Si and C of the samples heated at: a) 1000°C for 10h, b) 1100°C for 2h, and c) 1200°C for 2h.

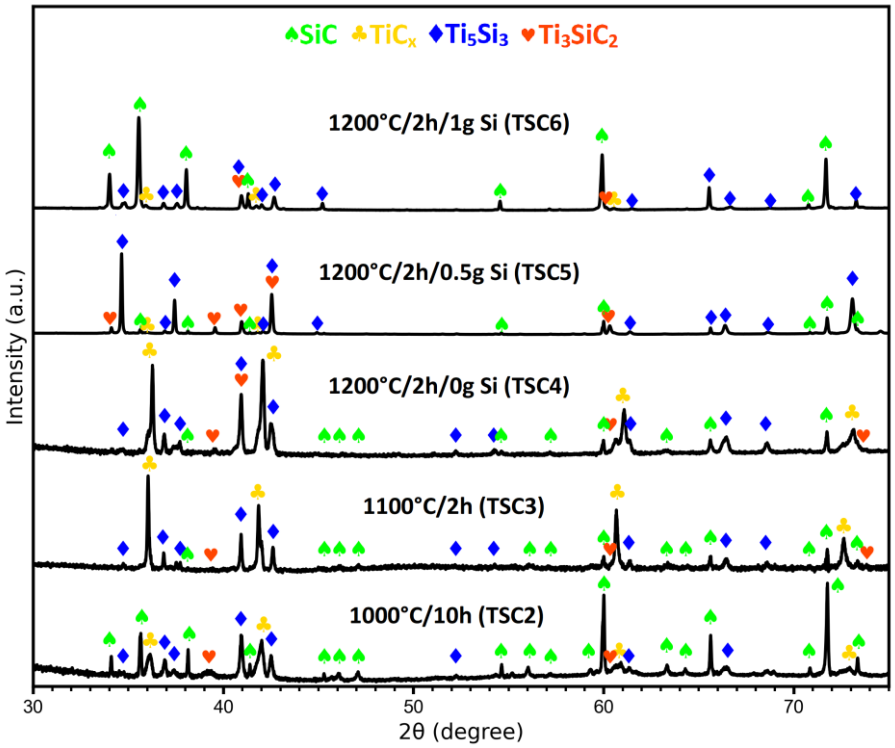

Figure 5. XRD patterns of the coatings and remaining powders from molten salts synthesis at 1000°C, 1100°C, and 1200°C.

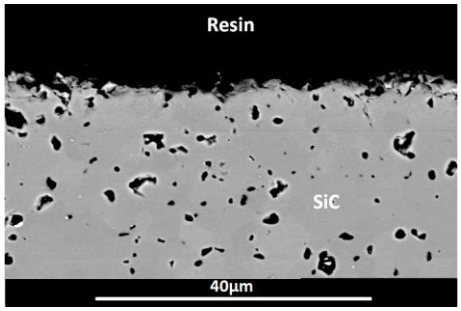

Figure 6. BSE image of the sample heated during 2h at 1200°C in the only presence of NaCl (SC).

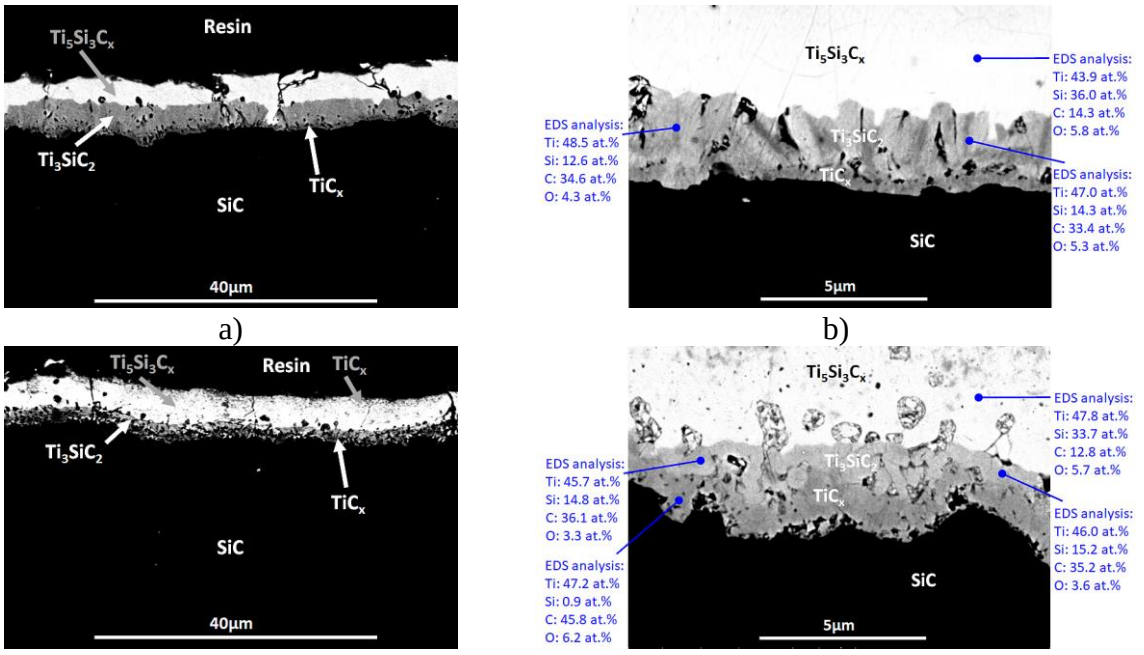

Figures 7. BSE images of the samples heated during 2h at 1200°C for two magnifications: a) x2000 and b) x10000 with addition of 0.5g of Si (TSC5); c) x2000 and d) x10000 with addition of 1g of Si (TSC6).

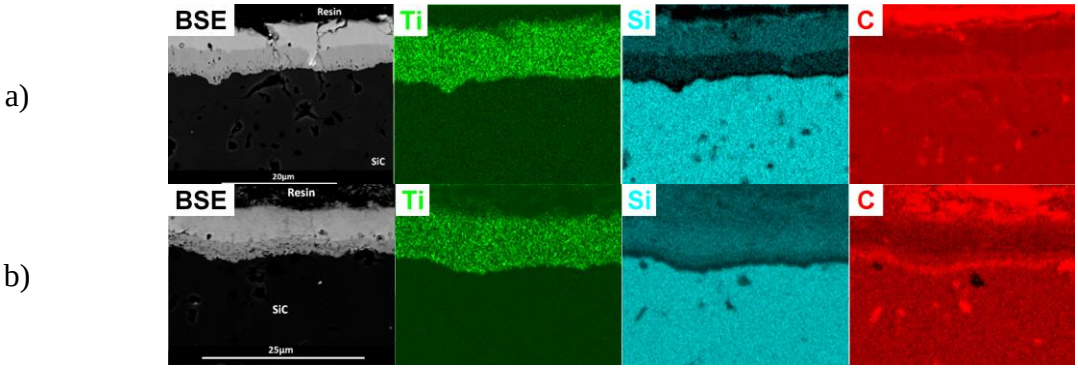

Figures 8. Backscattered electron micrograph and EDS mapping for Ti, Si and C of the SiC monoliths heated at 1200°C for 2h: a) with addition of 0.5g of Si; and b) with addition of 1g of Si.

a)

b)

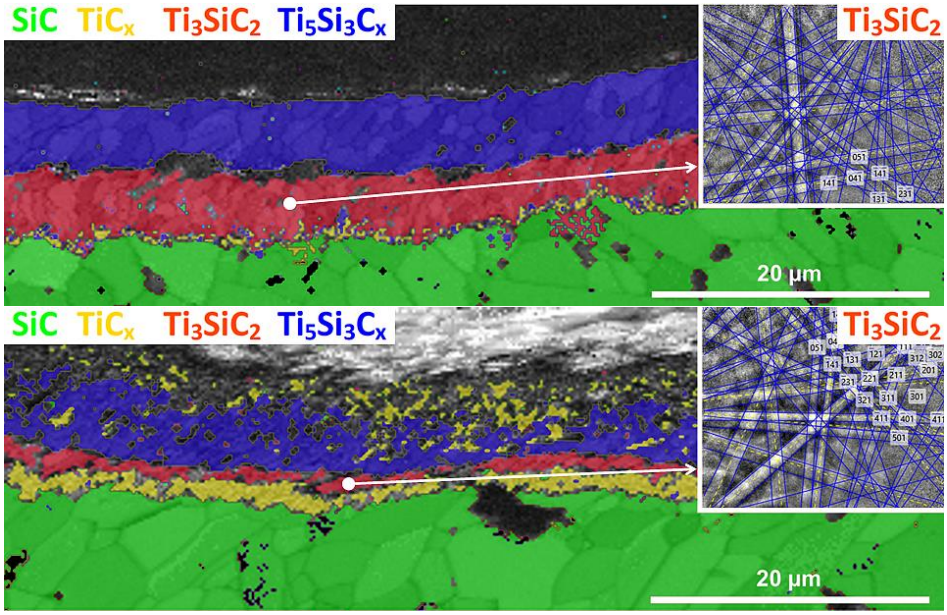

Figures 9. EBSD phases maps and examples of Ti_3SiC_2 band indexing in Kikuchi patterns in inset: a) with addition of 0.5g of Si (TSC5) and b) with addition of 1g of Si (TSC6).

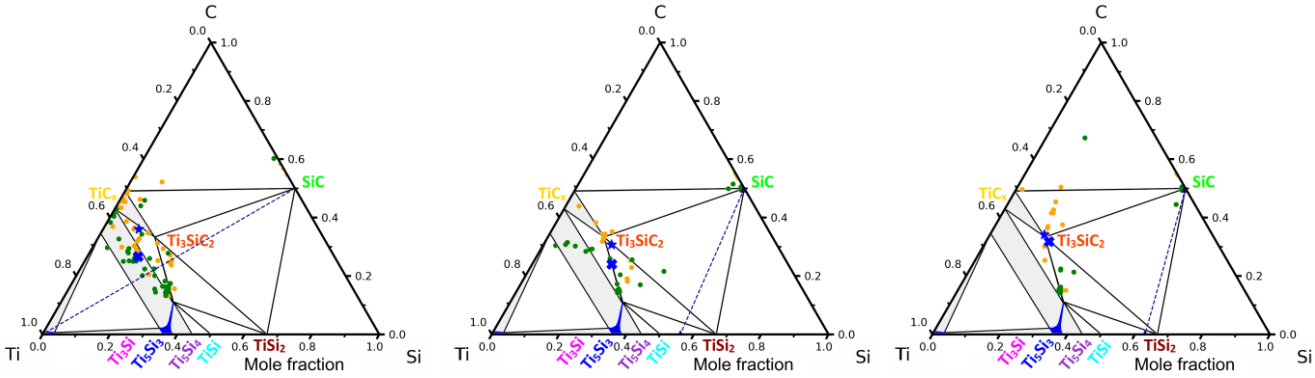

a) b) c)

Figures 10. Localization in the Ti-Si-C phase diagram of the EDS (orange points) and WDS (green points) measurements on SiC monoliths heated at 1200°C for 2h: a) without Si addition; b) with addition of 0.5g of Si; and c) with addition of 1g of Si. The mean compositions are localized by blue five-pointed stars (EDS) and blue saint Andrew's crosses (WDS).

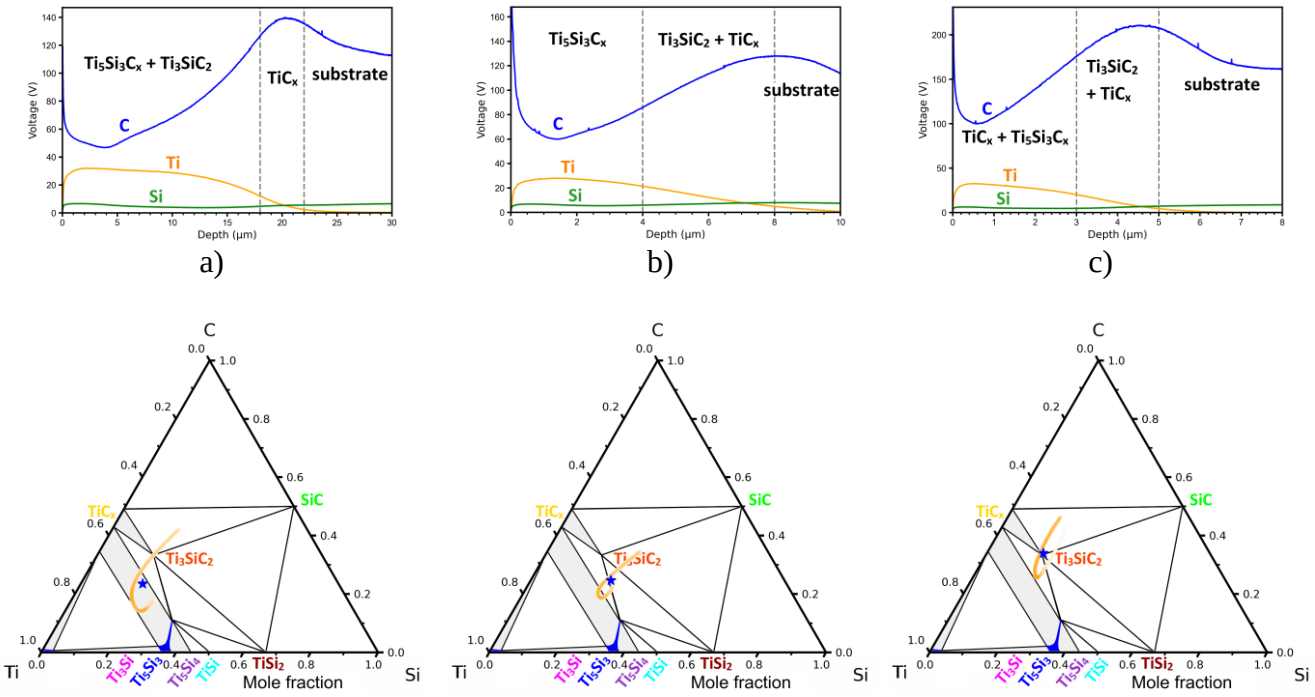

Figures 11. GDOES profiles measured on SiC monoliths heated at 1200°C for 2h: emission profile: a) without Si addition; b) with addition of 0.5g of Si; and c) with addition of 1g of Si; and atomic quantification: d) without Si addition; e) with addition of 0.5g of Si; and f) with addition of 1g of Si. The mean compositions are localized by blue five-pointed stars.

Table 1: Samples considered in this study.

Samples	Heat treatment	Mixture composition (g)			Coating thickness (µm)
		Ti	Si	NaCl	
TSC1	1000°C / 2h	1	-	6.27	0.5±0.1
TSC2	1000°C / 10h	1	-	6.27	8±1
TSC3	1100°C / 2h	1	-	6.27	9±1
TSC4	1200°C / 2h	1	-	6.27	20±1
TSC5	1200°C / 2h	1	0.5	6.27	7.0±0.5
TSC6	1200°C / 2h	1	1	6.27	5.0±0.5
SC	1200°C / 2h	-	-	6.27	0

Table 2: ICP quantifications of the residual powder after dissolution in water.

Sample		Ti	Si	C	O	Others
TSC4	Mass%	63.7	13.2	0.5	5.2	17.4
(1200°C/2h/0g Si)	At.%	61.3	21.7	1.9	15.0	-
TSC6	Mass %	45.2	38.1	0.6	8.2	7.9
(1200°C/2h/1g Si)	At.%	32.9	47.5	1.7	17.9	-